Novel UWB Transceiver for WBAN Networks: A Study on AWGN Channels

Chengshi Zhao, Zheng Zhou, and Kyungsup Kwak

A novel ultra-wideband (UWB) transceiver structure is presented to be used in wireless body area networks (WBANs). In the proposed structure, a data channel and a control channel are combined into a single transmission signal. In the signal, a modulation method mixing pulse position modulation and pulse amplitude modulation is proposed. A mathematical framework calculating the power spectrum density of the proposed pulse-based signal evaluates its coexistence with conventional radio systems. The transceiver structure is discussed, and the receiving performance is investigated in the additive white Gaussian noise channel. It is demonstrated that the proposed scheme is easier to match to the UWB emission mask than conventional UWB systems. The proposed scheme achieves the data rate requirement of WBAN; the logical control channel achieves better receiving performance than the logical data channel, which is useful for controlling and maintaining networks. The proposed scheme is also easy to implement.

Keywords: Wireless body area network, ultra-wideband, pulse position modulation, pulse amplitude modulation.

Manuscript received Dec. 30, 2008; revised Sept. 15, 2009; accepted Oct. 1, 2009.

This research was supported by the MKE (Ministry of Knowledge Economy), Korea, under the ITRC (Information Technology Research Center) support program supervised by the IITA (Institute for Information Technology Advancement) (IITA-2009-C1090-0902-0019).

Chengshi Zhao (phone: +82 32 864 8935, email: zhaochengshi@gmail.com) is with the UWB-ITRC, Graduate School of Information Technology and Telecommunications, Inha University, Incheon, Rep. of Korea, and also with the Wireless Network Laboratory, Beijing University of Posts and Telecommunications, Beijing, China.

Zheng Zhou (email: zzhou@bupt.edu.cn) is with the Wireless Network Laboratory, Beijing University of Posts and Telecommunications, Beijing, China.

Kyungsup Kwak (email: kskwak@inha.ac.kr) is with the UWB-ITRC, Graduate School of Information Technology and Telecommunications, Inha University, Incheon, Rep. of Korea.

doi:10.4218/etrij.10.0108.0738

I. Introduction

Ultra-wideband (UWB) is a radio technology that can be used at very low energy levels for short-range high-speed communications using a large bandwidth (>500 MHz). UWB radio devices share spectrum with existing narrowband transmissions without causing undue interference [1]-[3].

A wireless body area network (WBAN) consists of a set of mobile and compact intercommunicating sensors which are either wearable or implantable into the human body. These can continuously monitor vital body conditions and movements, such as diabetes, asthma, and heart attacks. These devices communicate through wireless technologies and transmit data from the body to a home base station. From there, data can be forwarded to a hospital, clinic, or elsewhere in real time [4]-[7]. WBAN technology is still in its initial stage and is being widely researched. The technology is expected to be a breakthrough in healthcare, and it is at the leading edge in implementing concepts such as "telemedicine."

UWB technology has been proposed for WBAN by the IEEE 802.15.6 task group [8]. The main application field of WBAN centers on the human body, a spectrum sensitive environment which requires low radiation. The sensors should be small. They are expected to be wearable or even implantable in human bodies; therefore, they can only support batteries with limited capacity. All of these factors make UWB an ideal technology for WBAN applications due to its low radiation power, high power efficiency, and most importantly, its high data rate in a small transmission range.

In [9], frequency modulation (FM) UWB (a special UWB technique using low modulation index frequency shift keying, followed by high-modulation index analog FM to achieve a wide bandwidth [10]) is proposed as a physical layer technique

for low-data-rate (LDR) transmission in WBAN. In [11], impulse radio (IR) UWB was proposed for LDR and medium-data-rate (MDR) transmissions in WBAN. The proposal for LDR refers to the standard of IEEE 802.15.4a which supports non-coherent energy detectors with low complexity. An enhanced mode, concatenated burst modulation, was proposed to resolve the problems of the low duty-cycle ratio and high inter-symbol interference for MDR situations. In [12], ETRI and Samsung Electronics jointly proposed a block-coded group pulse position modulation (PPM) scheme to be used in WBAN. This supports a non-coherent receiver. The modulation is independent of the pulse-shape. In [13], Texas Instruments proposed a physical layer technique called burst position modulation with time hopping (TH). It improves the symbol structure and time-hopping sequence over IEEE 802.15.4a. In [14], the National Institute of Information and Communications Technology (NICT) proposed a chirp-pulse-based IR-UWB physical layer. It has a coherent detector performing close to the full rake receiver with low complexity and low power consumption. In this, the timing resolution requirement of the coherent operation is close to the non-coherent short pulse IR-UWB with low sampling rate and low sampling resolution requirement. In [15], the NICT proposed a design based on IEEE 802.15.4a with a special signal format that supports coherent and non-coherent transceivers.

In this paper, which focuses on the IR-UWB transmission scheme, we propose a novel modulation method mixing PPM and pulse amplitude modulation (PAM) (binary phase shift keying (BPSK)-type PAM). The proposed modulation scheme defines two logical channels, namely, the logical data channel (LDCH), which carries signals that are PPM modulated, and the logical control channel (LCCH), which carries signals that are PAM modulated. Both the LCCH and the LDCH achieve the same receiving performance as the traditional PPM-UWB systems. Furthermore, the signals in the LCCH perform much better than the signals in the LDCH. Thus, the LCCH channel is suited to control and maintain WBAN networks. The LDCH and the LCCH are combined into a single transmission signal in the physical layer based on the proposed modulation type. Thus, the transmission for both the data and the signal control can be implemented in a single signal, while a special transceiver used to transmit a control signal in WBAN is retrenched. Analysis and simulation demonstrate that the proposed modulation scheme has a good (flat) power spectrum density (PSD) that can easily match the Federal Communication Commission's (FCC's) UWB emission mask. The proposed modulation scheme may be further combined with other IR-UWB-based proposals for WBAN [11]-[16] because the proposed scheme is independent of pulse shaping.

The remainder of this paper is organized as follows. Section II describes the signal formation for the followed discussions. The PSD of the signal is analyzed in section III. Novel transmitter and receiver structures are presented in section IV. Section V analyzes the receiving performance of the proposed mechanism. The simulation results are presented and discussed in section VI. Finally, section VII concludes the paper and mentions our intended future work.

II. Signal Formation

This section introduces the format of the proposed transmission signal. A similar format was presented in [17], but our proposal has some modifications. This will be described in two parts. First, a traditional PPM-TH UWB signal is used as the LDCH in WBAN networks to transmit the information at high speed and with restricted interference. Second, Miller-coded signals, which have a narrow bandwidth, are PAM modulated onto the PPM-TH UWB signals, and this is used as the LCCH in WBAN networks.

1. Signal in LDCH

The PPM-TH UWB signal adopted in the LDCH is a sequence of short pulses, that is, monocycles. A monocycle is usually a Gaussian-shaped pulse of finite duration T_p. It is zero out of the time span [0, T_p]. The duration is in the order of nanoseconds, which yields a bandwidth in the order of GHz.

Figure 1 shows the waveform employed in IR-UWB to transmit a single bit. The waveform of one bit is constituted by N_s monocycles and has a duration of T_b. The waveform of each bit is divided into N_s frames whose durations are T_s (T_s=T_b/N_s). Each frame is further divided into N_c chips with a chip duration of T_c (T_c=T_s/N_c). Based on the TH code, a monocycle is placed in a randomly selected chip in each frame. In the PPM

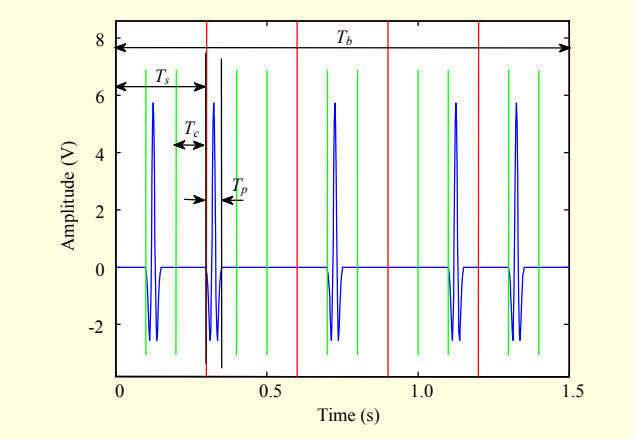

Fig. 1. Example of the LDCH (1 bit), where T_b=5T_s, T_s=3T_c, and T_c=2T_p=2ε. That is, N_s=5, N_c=3, and T_p=ε.

modulation type, the position of the monocycle inside a chip represents the input bit. We denote the position shift factor as ε ($\varepsilon<T_c$). Specifically, binary PPM is considered in this paper, so we set $\varepsilon=0$ if the input bit is zero, while $\varepsilon=T_p$ if the input bit is 1. PPM-caused overlaps between neighboring monocycles are not considered ($T_c \geq 2T_p$).

Therefore, the waveform employed to transmit the j-th bit of user u can be compactly written as

$$w_j^{(u)}(t) = w(t) \times \sum_{m=1}^{N_s} \delta(t - mT_s - C_m^{(u)} T_c - b_j^{(u)} \varepsilon),$$

where $b_j^{(u)}$ denotes the j-th bit of user u, $C_m^{(u)}$ denotes the TH code for the m-th frame in a transmission bit of user u, $*$ is the convolution operator, and $w(t)$ is the waveform of a monocycle. Correspondingly, the transmitted sequence of user u is expressed as

$$w^{(u)}(t) = \sum_{j=-\infty}^{\infty} w(t - jT_b) \times \sum_{m=1}^{N_s} \delta(t - mT_s - C_m^{(u)} T_c - b_j^{(u)} \varepsilon). \quad (1)$$

2. Signal in LCCH

In our proposal, a Miller-coded control channel signal is PAM modulated onto the LDCH signal. This is called the LCCH. Specifically, Miller-coded signals are produced for every bit of the LCCH, which is further PAM modulated. The modulated signal is used to multiply the corresponding LDCH monocycles.

Since the bit duration of the LDCH is T_b, the data rate of the LDCH is $1/T_b$; since the data rate of the LCCH is normally lower than that of the LDCH, we set $1/(T_b \times N_a)$ as the data rate of the LCCH. The bit duration of the control channel is $T_a = T_b \times N_a$, correspondingly. Figure 2 shows an example of the combined signal of the LDCH and the LCCH.

The waveforms are built up by monocycles that are modulated by PPM with PAM (BPSK-type), where PPM carries the LDCH information, and PAM carries the Miller encoded LCCH information. The bits in the LDCH and the bits in the LCCH are independent, so the modulation of PPM and that of PAM are independent as reflected in Fig. 2.

The value of N_a should be large to obtain some advantages. However, the data rate of the control channel will decrease if N_a is large; so there is a tradeoff to determine its value. This problem will be discussed later. From the preceding descriptions, we get that T_a and T_b are unequal, thus our proposal is different from the scheme of direct-sequence IR described in [17].

We choose the Miller code as a baseband encoding scheme in the LCCH since Miller encoding has the capability to carry timing information, and it has strong anti-interference capability. Another important advantage that is of interest to us is that it can transmit one bit in a narrower bandwidth compared to other baseband coding methods. That is, it has a higher spectral efficiency compared to other methods [18].

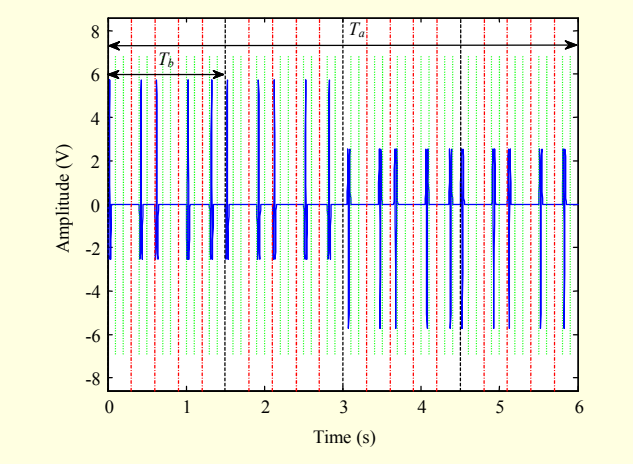

Fig. 2. Example of a combined signal (1 LCCH bit with 4 LDCH bits), where $T_a=4T_b$. There is a polarity inversion in the middle of the LCCH bit. (The inversion may be at the boundary of the bit according to Miller encoding rules.)

After Miller encoding, we denote the i-th bit of user u in the LCCH as $a_i^{(u)}$. Since one input bit is coded into two output bits by Miller encoding, $a_i^{(u)}$ has the same duration as $N_a/2$ bits in the LDCH. Finally, considering (1), we express the transmission sequence of user u as

$$w^{(u)}(t) = \sum_{i=-\infty}^{\infty} a_i^{(u)} w(t - i\frac{T_a}{2}) \times \sum_{j=0}^{N_a/2-1} \sum_{m=0}^{N_s-1} \delta(t - jT_b - mT_s - C_m^{(u)} T_c - b_{i,j}^{(u)} \varepsilon), \quad (2)$$

where $a_i^{(u)}$ is the i-th bit of the LCCH, and $b_{i,j}^{(u)}$ is the j-th bit of the LDCH in the duration of the i-th bit of the LCCH; the rate matching of these two channels should be ensured during modulation.

As shown in the equation, the information in the LCCH is PAM modulated, while the information in the LDCH is PPM modulated. Equation (2) is the combined signal of the LDCH and the LCCH. The signals of the LDCH and the LCCH are combined into a single transmission signal through modulation.

III. Spectrum Analyses

In this section, the PSD of the proposed scheme is analyzed, and the receiver structure is introduced.

1. Transmutative Description

The signals from different channels are considered to be independent to make the discussion on PSD straightforward.

$$w^{(u)}(t) = w_C^{(u)}(t) \times w_D^{(u)}(t), \tag{3}$$

where $w_C^{(u)}(t) = \sum_{c=-\infty}^{\infty} w_C^{(u)}(t - cT_a)$ is the LCCH signal, and $w_D^{(u)}(t)$ is the LDCH signal. The signal in (2) is the combined signal which is composed of pulses (monocycles). In (3), only $w_D^{(u)}(t)$ represents pulses (monocycles), and $w_C^{(u)}(t)$ is the Miller-coded polar-indication signal without any pulse expression imbedded. The overall signal is a product of these two signals.

2. PSD Calculation

Specifying one user, the Fourier transform of (3) is given by

$$W(f) = W_C(f) \times W_D(f), \tag{4}$$

where $W_C(f)$ is the LCCH PSD, and $W_D(f)$ is the LDCH PSD (PPM-TH UWB). Based on [19] and [2], $W_C(f)$ and $W_D(f)$ are respectively obtained:

$$\begin{aligned} W_C(f) = {} & \frac{2}{(2\pi f)^2 T_a [17 + 8\cos\theta]} \\ & \times [23 - 2\cos\theta - 22\cos 2\theta - 12\cos 3\theta + 5\cos 4\theta \\ & + 12\cos 5\theta + 2\cos 6\theta - 8\cos 7\theta + 2\cos 8\theta], \end{aligned} \tag{5}$$

where $\theta = \pi f T_a$. The increase of T_a causes the bandwidth of $W_C(f)$ to decrease and the peak value of $W_C(f)$ to increase.

$$W_D(f) = \frac{|W_v(f)|^2}{T_b} \left[\sin^2(\pi f \varepsilon) + \frac{\cos^2(\pi f \varepsilon)}{T_b} \sum_{n=-\infty}^{\infty} \delta(f - \frac{n}{T_b}) \right], \tag{6}$$

where $W_v(f) = W_0(f) \sum_{m=1}^{N_s} e^{-j(2\pi f(mT_s + C_m T_c))}$, and $W_0(f)$ is the PSD of a monocycle.

The PSD of the proposed signal is obtained by convolving $W_C(f)$ with the continuous and discrete components of (6).

Convolving $W_C(f)$ with the continuous component of (6) results in

$$W_1(f) = W_C(f) \times \left[\frac{|W_v(f)|^2}{T_b} \sin^2(\pi f \varepsilon) \right]. \tag{7}$$

According to (5) and (6), the decisive factors of the bandwidth of $W_C(f)$ and $W_v(f)$ are T_a and T_p, respectively. Since T_a is much larger than T_p, $W_C(f)$ is a narrow band signal compared with $W_v(f)$. Therefore, the bandwidth and the shape of $W_1(f)$ remain almost the same as those in $W_v(f)$. Only the amplitude of $W_1(f)$ is affected by $W_C(f)$. This is not the most important consideration here. We draw the conclusion that the PSD of the proposed signal is still an IR-UWB PSD whose power mainly focuses on $[0, 5/T_p]$.[1] This implies that the bandwidth of the proposed scheme is $5/T_p$.

Convolving $W_C(f)$ with the discrete component of (6) results in

$$\begin{aligned} W_2(f) &= \left[\frac{|W_v(f)|^2}{T_b} \frac{\cos^2(\pi f \varepsilon)}{T_b} \sum_{n=-\infty}^{\infty} \delta(f - \frac{n}{T_b}) \right] \times W_C(f) \\ &= \frac{1}{T_b^2} \sum_{n=-\infty}^{\infty} \left| W_v(\frac{n}{T_b}) \right|^2 \cos^2(\pi \frac{n}{T_b} \varepsilon) W_C(f - \frac{n}{T_b}). \end{aligned} \tag{8}$$

According to (8), the LCCH PSD is conveyed to $f=n/T_b$ with some amplitude scaling. Obviously, it is symmetrical at $f=n/T_b$. For the amplitude scaling, we have

$$\frac{1}{T_b^2} \left| W_v(\frac{n}{T_b}) \right|^2 \cos^2(\pi \frac{n}{T_b} \varepsilon) = \frac{1}{T_b^2} \left| W_0(\frac{n}{T_b}) \right|^2 \left| \sum_{m=1}^{N_s} e^{-j(2\pi \frac{n}{T_b}(mT_s + C_m T_c))} \right|^2 \cos^2(\pi \frac{n}{T_b} \varepsilon),$$

where $W_0(f)$ is the PSD of a monocycle, and it is almost constant in the bandwidth of $[0, 5/T_p]$. The term (9) obtains a considerable peak value only if $n=kT_b/T_p$, where $k \in \{1, 2, 3, \cdots\}$:

$$\frac{1}{T_b^2} \left| \sum_{m=1}^{N_s} e^{-j(2\pi \frac{n}{T_b}(mT_s + C_m T_c))} \right|^2 \cos^2(\pi \frac{n}{T_b} \varepsilon). \tag{9}$$

Substituting $n=kT_b/T_p$ into $f=n/T_b$, we determine that notable PSD peaks exist in the spectral positions of $f=k/T_p$. This means that the LCCH information is conveyed to the spectral positions of $f=k/T_p$ with considerable power, while the power is small and negligible in other spectral positions. We know that the main power of the Gaussian-shaped UWB signal focuses on $[0, 5/T_p]$. Thus, we conclude that the LCCH information mainly exists at $f=k/T_p$, where k=1, 2, 3, 4, and 5.

3. Numerical Results

Simulation is performed to reflect the PSD performance of the proposed signal. The simulation parameters are listed in Table 1. Figure 3 shows the simulation results.

Figures 3(a) and (b) show the PSD performance of $W_C(f)$. No discrete component is included in $W_C(f)$, and the spectral efficiency is about 2 bit/s/Hz. According to (5), the bandwidth of $W_C(f)$ decreases, and the peak value of the PSD increases when T_a increases.

The peaks of the PSD appear at 2 GHz, 4 GHz, 6 GHz, and 8 GHz in Fig. 3(d) (The PSD is too small to be considered for the spectral position of 10 GHz.), while these spectral positions are all deep fadings in Fig. 3(c). This verifies the conclusion in section III.2; the LCCH information mainly exists at $f=k/T_p$, where k=1, 2, 3, 4, and 5.

1) This conclusion is achieved by the PSD of the Gaussian pulse-based UWB system. However, the proposed system can be similarly expanded to systems that adopt different pulse shapes.

Table 1. Simulation parameters.

T_a (s)	3*e*–7
T_b (s)	1.5*e*–8
T_c (s)	1*e*–9
T_p (s)	5*e*–10
T_s (s)	3*e*–9
ε (s)	5*e*–10
Sampling rate	5*e*10
Average transmitted power	–30 dBm

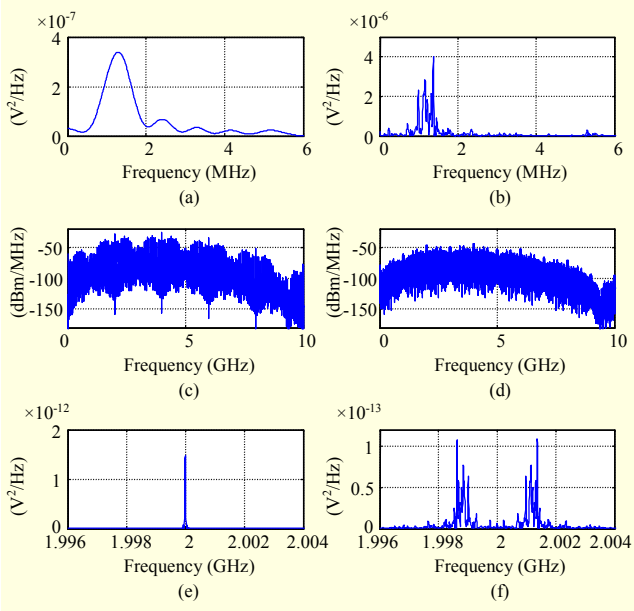

Fig. 3. PSD Simulations: (a) theoretical PSD of $W_C(f)$, (b) simulated PSD (N_a=20) of $W_C(f)$, (c) PPM-TH UWB PSD, (d) proposed scheme PSD, (e) specified PPM-TH UWB PSD around 2 GHz, and (f) specified PSD of the proposed scheme around 2 GHz.

Figures 3(e) and (f) specify the PSD around 2 GHz for PPM-TH UWB and the proposed scheme, respectively. The discrete components of Fig. 3(e) are replaced by continuous components in Fig. 3(f). Further comparing Figs. 3(b) and (f), we determine that the LCCH information is exactly carried around 2 GHz, where it is a useless discrete component for PPM-TH UWB in Fig. 3(e). This is also in accord with the conclusion in section III.2.

Therefore, we conclude that there is a high discrete PSD for PPM-TH UWB, and with a large proportion of discrete PSD that does not carry any useful information, a lot of power of the traditional PPM-TH UWB is wasted. This is a crucial threat to the FCC's emission mask. In the proposed scheme, most of the discrete PSD is restrained, and some discrete PSD is replaced by the useful information of the LCCH. This increases the power efficiency and makes it easier to satisfy the FCC's UWB emission mask requirement.

IV. Transceiver Description

This section introduces the transceiver structure for the proposed scheme, where the optimal receiver in the additive white Gaussian noise (AWGN) channel is specialized.

1. Transmitter

Considering the transmitter structure of PPM-TH UWB, we describe the proposed transmitter as shown in Fig. 4.

As for the LDCH, the input bit sequence is generated at a rate of R_b=1/T_b. Each bit is repeated N_s times by the repetitive encoder which represents the frames constructing the bit. In the transmission encoder module, a position shift for each pulse is generated.

As for the LCCH, the binary input sequence is generated at a rate of R_b=1/T_b. In the Miller encoder module, the data rate of two channels should be matched, implying that T_a=N_a×T_b=N_a×N_s×T_s. Here, N_s is related to the receiving performance of the LDCH, N_a is determined by the difference between the data rates of the LCCH and the LDCH, and the relationship between these two data rates is expressed as R_{LDCH}=N_a×R_{LCCH}. The PSD of the transmitted signal is related to N_a as described in section III.2. An increase of N_a will cause T_a to increase. This results in an increase in the peak value of the PSD. Furthermore, the receiving performance of the LCCH, which will be discussed later, is also related to N_a. Therefore, the tradeoff of the difference between R_{LDCH} and R_{LCCH}, the PSD of the transmitted signal, and the receiving performance of the LCCH should be jointly considered to determine the value of N_a.

The multiplier between two channels can be realized by a non-real multiplier. The signal of the LCCH is not like the signal of the LDCH, whose signal is composed of pulses; instead, it is a continuous direct current signal with some polarity inversions. Thus, when multiplication is executed, we can simply use the signal of the LCCH as a reference signal. If the reference is negative, the pulses in the LDCH reverse the phase; otherwise, they do nothing.

2. Receiver

It is assumed that the signal is transmitted in a zero mean and N_0/2 variance AWGN channel without multiuser interference. The received signal is $R(t)$=$w(t)$+$n(t)$, where $w(t)$ is the transmitted signal, and $n(t)$ is the AWGN noise. If the channel fading is included in the considerations, we have $R(t)$=$\rho w(t)$+$n(t)$, where ρ is the fading factor. Assume that the effects of both the transmitter and receiver antennas on the

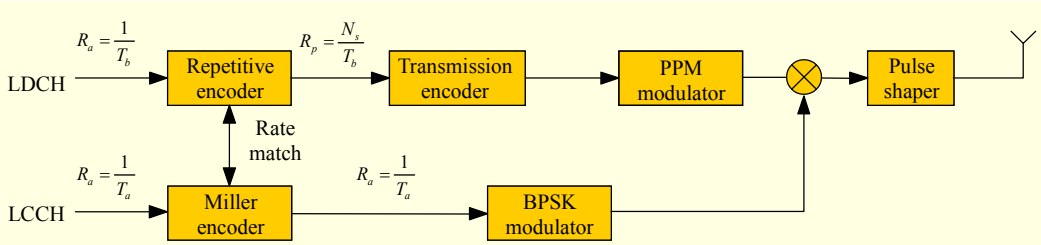

Fig. 4. Transmitter structure for proposed scheme.

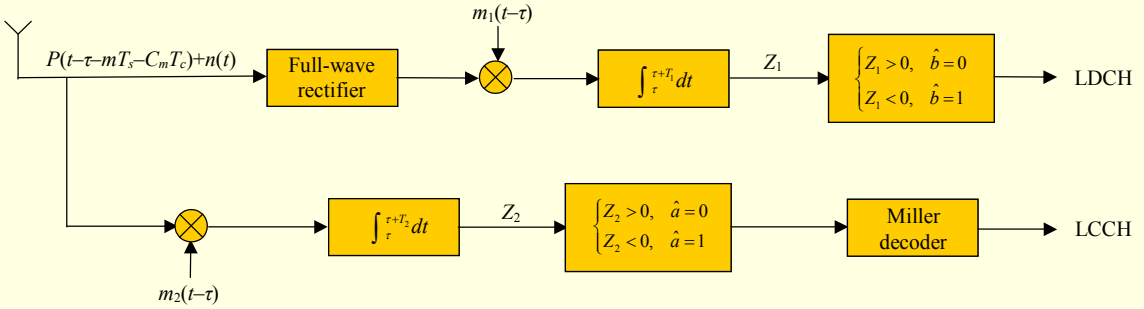

Fig. 5. Receiver structure for the proposed scheme: $T_1=T_2=T_s$ for hard decision and $T_1=T_b$, $T_2=T_a/2$ for soft decision.

shape of the pulses are already perfectly considered in the pulse shaper on the transmitter side. We propose the optimal receiver structure shown in Fig. 5.

In our considerations, we assume that the synchronization is perfectly done. This means that T_a, T_b, T_s, T_c, T_p, and C_m are all known on the receiver side. Two decision rules are explained in the receiver side, namely, hard decision and soft decision.

A. Hard Decision

The correlation template for hard decision is composed of pulses during one frame time. Thus, the receiving templates for the LDCH and the LCCH are set as $m_1(t)$ and $m_2(t)$, respectively:

$$m_1(t) = w_0(t-\tau-C_mT_c) - w_0(t-\tau-C_mT_c-\varepsilon),$$
$$m_2(t) = w_0(t-\tau-C_mT_c) + w_0(t-\tau-C_mT_c-\varepsilon),$$

where $w_0(t)$ is an energy-normalized frame.

For the LDCH to decide one bit, N_s pulses that represent one bit are decided independently, and the final result is obtained from the N_s decision results using a simple majority criterion. Similarly, for the LCCH to decide one bit, $N_a/2\times N_s$ pulses that represent one Miller-coded bit are decided independently. Decision is performed frame by frame in hard decision, in which only one pulse is included.

B. Soft Decision

For the LDCH, the correlation template for soft decision is composed of N_s pulses in the duration of one received bit:

$$m_1(t) = N_s^{-\frac{1}{2}} \sum_{m=1}^{N_s} \left[w_0(t-\tau-C_mT_c) - w_0(t-\tau-C_mT_c-\varepsilon) \right].$$

In soft-decision-based detection, each bit composed of N_s frames is considered by the receiver as a multipulse signal. The received signal is cross-correlated with the receiver template that is matched to the train of pulses representing the corresponding bit. The decision is performed bit by bit.

Similarly, the correlation template for soft decision is composed of $N_a/2\times N_s$ pulses for the LCCH in the duration of each received Miller-coded bit:

$$m_2(t) = N_d^{-\frac{1}{2}} \sum_{m=1}^{N_d} \left[w_0(t-\tau-C_mT_c) + w_0(t-\tau-C_mT_c-\varepsilon) \right],$$

where $N_d = N_a/2\times N_s$.

Figure 6 demonstrates the templates for different kinds of receivers. The receiving template is the same as traditional PPM-TH UWB for the LDCH, and the received signal is the same as traditional PPM-TH UWB system after passing through the full-wave rectifier. For the LCCH, the receiver template is different from traditional PAM UWB because the received signal is modulated by PAM with PPM, and the exact positions of pulses cannot be obtained. Thus, the receiver template simply repeats the pulse in two positions. This decreases receiving performance because the integrator with longer duration introduces more noise to the receiver. This will be analyzed later.

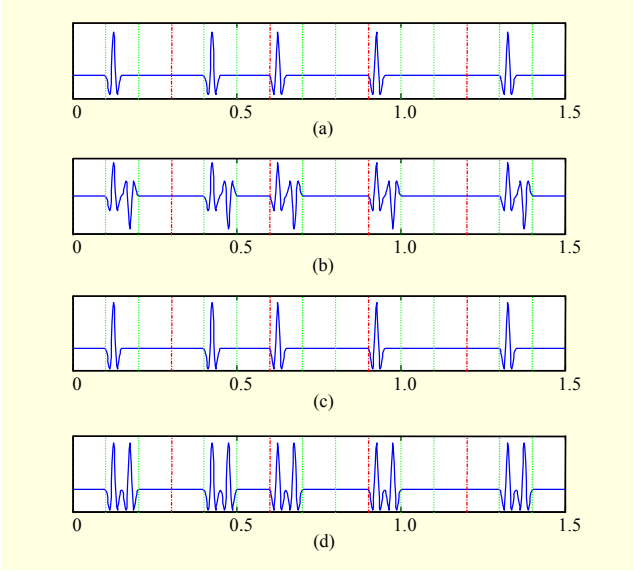

Fig. 6. Receiver templates for different UWB modulations: (a) transmitted signal, (b) template for LDCH (PPM-TH), (c) template for PAM-TH, and (d) template for LCCH.

V. Receiving Performance

In this section, receiving performance is analyzed in a zero mean and $N_0/2$ variance AWGN channel without multiuser interference.

1. LDCH

For the LDCH, since the decision is the same as that of the traditional PPM-TH UWB, receiving performance of soft decision in AWGN channel as in [2] is given as

$$P_{\mathrm{s}}^{\mathrm{DC}} = \frac{1}{2}\mathrm{erfc}\left(\sqrt{\frac{E_D}{2N_0}}\right) = \frac{1}{2}\mathrm{erfc}\left(\sqrt{\frac{N_s E_X}{2N_0}}\right), \qquad (10)$$

where $\mathrm{erfc}(x) = 2\pi^{-\frac{1}{2}}\int_x^{\infty} e^{-r^2}dr$, E_D is the received energy per LDCH bit, and E_X is the received energy per frame. By increasing the number of pulses per bit, the received energy is increased by a factor of N_s with a consequent reduction in the bit error rate (BER).

For hard decision, given the number of pulses falling over a threshold and comparing this number to the number of pulses falling below the same threshold, the estimated bit corresponds to the higher of these two numbers. An error occurs if more than half of the pulses included in a bit are misinterpreted, and the probability of the bit error is given by

$$P_{\mathrm{h}}^{\mathrm{DC}} = \sum_{i=\lceil \frac{N_s}{2} \rceil}^{N_s} C_{N_s}^{i} P_0^{i} (1-P_0)^{N_s - i}, \qquad (11)$$

where $P_0 = \frac{1}{2}\mathrm{erfc}\left(\sqrt{\frac{E_X}{2N_0}}\right)$ is the decision error rate of a frame.

2. LCCH

First, we would like to calculate the receiving performance for a single pulse in the LCCH. There are four possible received signals in the LCCH in the following equation:

$$S_{RX}(t) = \begin{cases} \sqrt{E_X}\, w_0(t), & a=1,\ b=0; \\ \sqrt{E_X}\, w_0(t-\varepsilon), & a=1,\ b=1; \\ -\sqrt{E_X}\, w_0(t), & a=-1,\ b=0; \\ -\sqrt{E_X}\, w_0(t-\varepsilon), & a=-1,\ b=1, \end{cases}$$

where a is the transmitted bit of the LCCH, and b is the transmitted bit of the LDCH. Using the template to achieve the correlation results, and after passing through the integrator, we obtain the following signal:

$$Z = S_{RX} + n_0,$$

where n_0 is a Gaussian random variable with zero mean and variance N_0[2)], and

$$S_{RX} = \begin{cases} \sqrt{E_X}, & a=1; \\ -\sqrt{E_X}, & a=-1. \end{cases}$$

For the equally probable and independent information bit, the average error probability can be expressed as

$$\begin{aligned} P_{a=-1\to a=+1} &= \frac{1}{2}\Pr(Z>0|b=1) + \frac{1}{2}\Pr(Z>0|b=0) \\ &= \Pr(Z>0|b=1) = \Pr\left(\sqrt{E_X} < n_0\right) \\ &= \frac{1}{2}\mathrm{erfc}\left(\sqrt{\frac{E_X}{2N_0}}\right). \end{aligned}$$

Total error probability is expressed as

$$P_0 = \frac{1}{2}P_{a=-1\to a=+1} + \frac{1}{2}P_{a=+1\to a=-1} = \frac{1}{2}\mathrm{erfc}\left(\sqrt{\frac{E_X}{2N_0}}\right). \qquad (12)$$

Similar to the LDCH case, it is easy to determine the error rate of the LCCH in soft decision:

$$P_{\mathrm{s}}^{\mathrm{CC}} = \frac{1}{2}\mathrm{erfc}\left(\sqrt{\frac{E_C}{2N_0}}\right) = \frac{1}{2}\mathrm{erfc}\left(\sqrt{\frac{N_s \times N_a \times E_X}{4N_0}}\right), \qquad (13)$$

where E_C is the received energy per LDCH bit, and E_X is the received energy per pulse.

It should be noted that the duration of the received bit is $T_a/2$ since the received bit is a Miller-coded bit whose duration is $T_a/2$, and $N_s \times N_a/2$ pulses are included in one received LCCH bit. The influence of Miller-decoding will be analyzed later.

2) Variance equals N_0 as follows: based on the proposed receiver template, n_0 here is an addition of two noise signals that are all zero mean and $N_0/2$ variance noises.

The error rate of the LCCH is the same as that of the LDCH if $E_C=E_D$. However, if we consider the receiving performance in the case of $E_C=N_a/2\times E_D$, we find that the receiving performance of the LCCH is much better than that of the LDCH in the system. This means that the receiving performance of the LCCH is better than that of the LDCH. Thus, it is useful for controlling and maintaining WBAN networks.

Similar to the LDCH case, receiving performance of the LCCH in the hard decision case can be obtained by

$$P_{\mathrm{h}}^{\mathrm{CC}} = \sum_{i=[\frac{N_s\times N_a}{4}]}^{\frac{N_s\times N_a}{2}} C_{N_s\times N_a/2}^{i} P_0^i (1-P_0^i)^{N_s\times N_a/2-i}. \quad (14)$$

3. Error Consideration for Miller Decoding

The error rate calculations in section V.2 only consider the error rate before Miller decoding. The influence of Miller decoding is considered as follows.

An input error in the Miller decoder will cause one error output bit by Miller decoding. As shown in Fig. 7(a), two neighboring error input bits cause two error output bits, while in another case, shown in Fig. 7(b), there will be no error output bit for two neighboring error input bits. These two cases have the same probability due to the randomness of the input errors in the Miller decoder. Therefore, the average error rate of Miller decoding is one bit for two neighboring error input bits.

Similarly, there is one bit decoding error for m continuous input errors, where $m \in \{1, 2, \cdots\}$. The decoding error probability can be expressed as

$$P' = P_1 + P_2 + P_3 + \cdots + P_m + \cdots, \quad (15)$$

where P_m is the decoding error rate for m continuous error input bits. Since m continuous error bits are composed of m continuous error bits with one correct bit at the each end of this error sequence, we find

$$P_m = (1-P)^2 P^m. \quad (16)$$

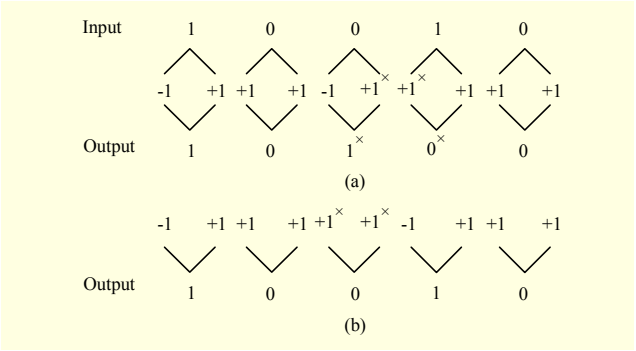

Fig. 7. Examples of 2 neighbor bit errors in Miller decoding.

Substituting (16) into (15), we find

$$P' = (1-P)^2 \prod_{m=1}^{\infty} P^m = (1-P)P. \quad (17)$$

Substituting the error rate expressions of (13) and (14) into (17), we can determine the final BERs of the LCCH for the case of soft and hard decisions, respectively.

VI. Numerical Results

This section presents simulation focusing on the BER performance of the proposed scheme. The simulation parameters are shown in Table 1. Unless otherwise specified, the hard decision scheme is adopted in the simulations.

The simulation results of the BER performance are shown in Fig. 8. The results verify (10) and (13), where the BER performance of the LDCH and the LCCH is the same if E_D/N_0

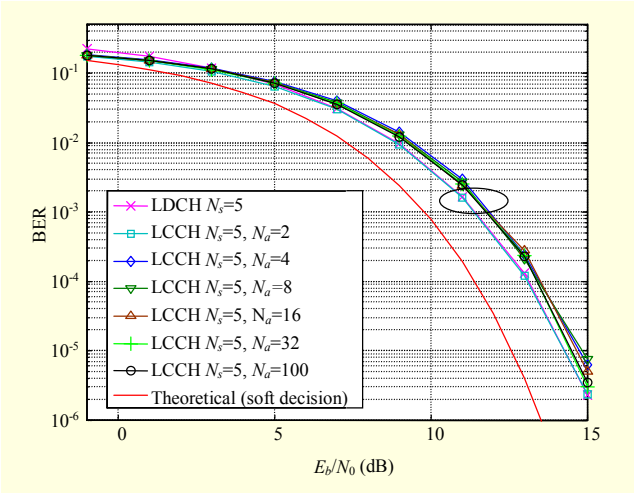

Fig. 8. BER comparison of different N_a (N_s=5).

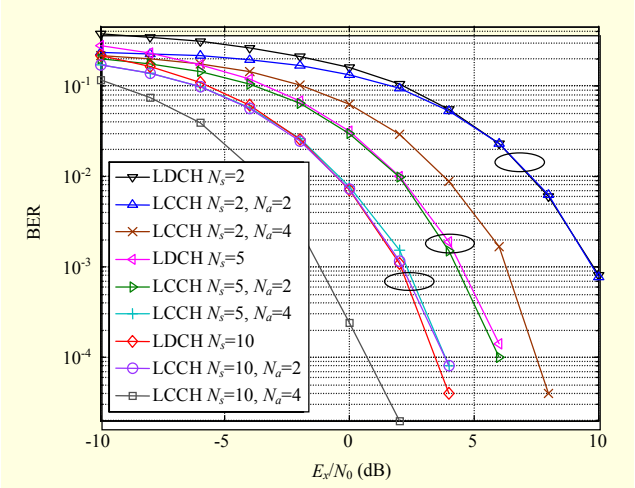

Fig. 9. BER comparison of different channels, where the LDCH has the same performance as PPM-TH UWB systems.

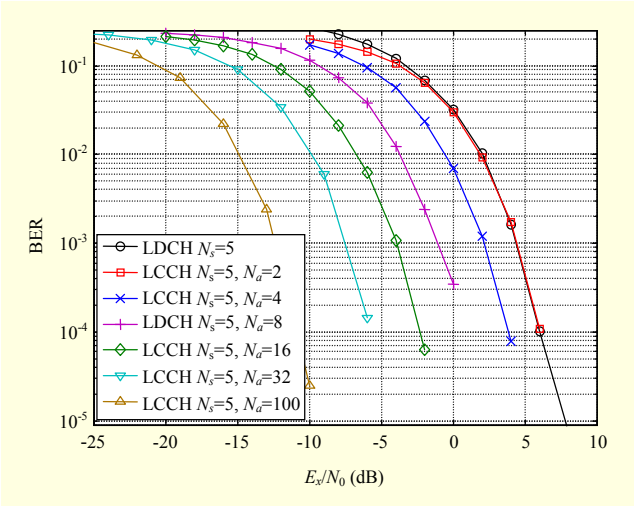

Fig. 10. BER comparison of different N_a (N_s=5).

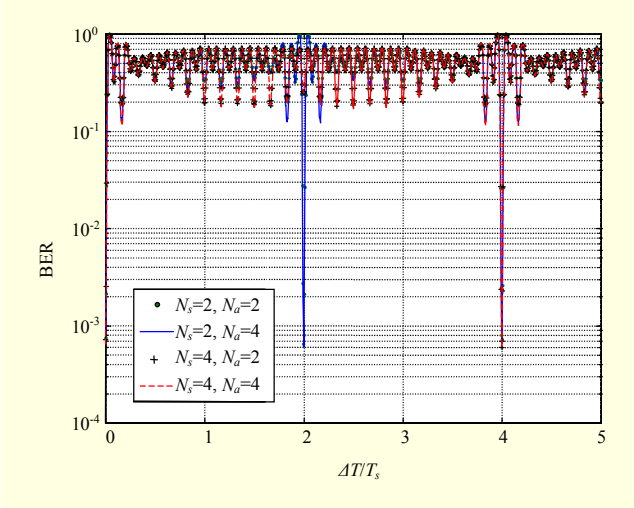

Fig. 11. BER declines caused by the normalized ΔT.

is equal to E_C/N_0 (In the figure, both E_D/N_0 and E_C/N_0 are denoted as E_b/N_0.). A theoretical curve of the soft decision case is shown in the figure to compare the performance of hard and soft decisions. As shown in the figure, the soft decision achieves a performance about 1.5 dB better than that of the hard decision. From the figure, we find that the proposed scheme achieves the same BER performance as traditional PPM-TH UWB systems.

According to the foregoing descriptions, $E_C=N_a/2\times E_D$ in the proposed scheme. Thus, the receiving performance of the LCCH is much better than that of the LDCH in the system. As seen in Fig. 9, where the X-axis is E_x/N_0 rather than E_b/N_0, the LCCH achieves a much better receiving performance than the LDCH under a given N_s. Furthermore, the LDCH and the LCCH achieve the same BER performance if N_s of the LDCH equals $N_s\times N_a/2$ of the LCCH. This means that the two

Table 2. Link budget (soft decision).

	High PSD	Low PSD	Calculation
Center freq. (MHz)	4,000	4,000	
BW (MHz)	500	500	A
Bit rate (bps)	10^7	10^4	B
Tx PSD (dBm/MHz)	–41.3	–70	D
Tx antenna gain (dBi)	0	0	E
EIRP (dBm)	–14.3	–43	F=D+10log$_{10}$A+E
Rx antenna Gain (dBi)	0	0	G
Path loss @ 3 m (dB)	62	62	H
Log-normal fading	6.5	6.5	I
C (dBm)	–82.8	–111.5	J=F+G–H–I
Thermal noise (dBm/Hz)	–174.1	–174.1	K
Noise figure (dB)	6	6	L
N_0 (dBm/Hz)	–168.1	–168.1	M=K+L
C/N_0 (dBHz)	85.3	56.6	N=J–M
E_b/N_0 (dB)	15.3	16.6	O=N–10log$_{10}$B
Required E_b/N_0 (dB)	12.6	12.6	P
Link margin (dB)	2.7	4	Q=O–P
Receiver sensitivity (dBm)	–85.5	–115.5	R=M+P+10 log$_{10}$B

channels have the same performance if the number of pulses included in one LDCH-bit is the same as the number of pulses included in the half-LCCH-bit. The reason is that the decision is performed in half the duration of one LCCH bit in the demodulator of the LCCH. The small difference between them is caused by Miller decoding; this is negligible at low BERs.

The influence of N_a on the BER performance is simulated in Fig. 10. Since the energy per pulse is the decisive factor of the average radiation power of the system, which is restricted by the FCC's emission mask, we still set E_x/N_0 as the X-axis to research the receiving performance. From the figure, we reach the conclusion that larger N_a, the better the performance that can be achieved by the LCCH.

From Figs. 9 and 10, we draw a similar conclusion to that in traditional UWB systems; the more pulses included in one bit, the better performance can be achieved. The number of pulses in one LDCH bit is N_s, and it is $N_s\times N_a$ in one LCCH bit. Therefore, the LCCH performs better than the LDCH, and the performance improves with the increase of N_a. Since the data rate of the LCCH is much smaller than the data rate of the LDCH (N_a>>1), the LCCH performs much better than the LDCH. With the same error rate, the LCCH can transmit further. This is useful to control and maintain the network.

To study the effect of imperfect synchronization on BER

performance, we designed a simulation whose results are shown in Fig. 11, where ΔT is the mistiming between transmitter and receiver. In the simulation, E_b/N_0 is set to be 10 dB. Correspondingly, the BER is 7.8×10^{-4} in soft decision case without time offset. Observing this figure, we find that the periodic decline of BER depends on the value of N_s, and it is independent of N_a. Timing offset has no influence on the BER performance when $\Delta T/T_s=l\times N_s$, $l\in\{0, 1, 2,\cdots\}$; however, the BER performance declines seriously in other cases. Therefore, synchronization is an important issue for further work on the proposed system.

The link budget of the proposed scheme is analyzed in Table 2, where a transmission distance of 3 m is specified. The target BER performance is 10^{-5} and the corresponding E_b/N_0 requirement is 12.6 dB in the soft decision case. Based on the FCC's UWB emission mask, two situations are analyzed. In case I, whose transmission PSD restriction is –41.3 dBm/MHz, a data rate of 10 Mbps can be achieved. In case II, whose transmission PSD restriction is –70 dBm/MHz, a data rate of 10 kbps can be achieved. These two data rates meet the requirement of WBAN.

VII. Conclusion and Future Work

In this paper, we proposed a novel transceiver structure for WBAN networks which can transmit data channel information together with control channel information in a single modulated signal. Using this scheme, original UWB signals are improved in the frequency domain; thus, the signal can meet the FCC's emission mask requirement more easily. Receiving performance of both the data channel and the control channel satisfy the transmission requirement of WBAN according to the link budget analyses. With the same receiving performance, information of the control channel can be transmitted further, which is useful to build up and maintain networks. Most of all, the proposed scheme is easy to realize. It is compatible with the existing IR-UWB systems, which is very suitable for WBAN sensor networks.

The proposed scheme can be expanded into multipath channels, such as classical UWB CM_1-CM_4 channels. It could be a valuable work to expand the proposed scheme into potentially standardized WBAN channels. These will be the aims of our future work.

References

[1] M.Z. Win and R.A. Scholtz, "Impulse Radio: How It Works," *IEEE Commun. Lett.*, vol. 2, no. 2, Feb. 1998, pp. 36-38.

[2] M.D. Benedetto and G. Giancola, *Understanding Ultra Wide Band Radio Fundamentals*, NJ, Prentice Hall PTR, June 2004.

[3] K. Siwiak and D. McKeown, *Ultra-wideband Radio Technology*, John Wiley, UK, 2004.

[4] E. Jovanov et al., "A WBAN System for Ambulatory Monitoring of Physical Activity and Health Status: Applications and Challenges," *Proc. IEEE EMBS*, 2005, pp. 3810-3813.

[5] C. Otto et al., "System Architecture of A Wireless Body Area Sensor Network for Ubiquitous Health Monitoring," *J. Mobile Multimedia*, vol. 1, no. 4, 2006, pp. 307-326.

[6] E. Jovanov et al., "A Wireless Body Area Network of Intelligent Motion Sensors for Computer Assisted Physical Rehabilitation," *J. Neuroeng. and Rehabil.*, vol. 2, no. 1, Mar. 2005, pp.1-10.

[7] E. Farella et al., "A Wireless Body Area Sensor Network for Posture Detection," *Proc. IEEE ISCC*, June 2006, pp. 454-459.

[8] https://mentor.ieee.org/802.15/documents?is_group=0006.

[9] J.F.M. Gerrits, J. Rousselot, and J.R. Farserotu, "CSEM FM-UWB Proposal Presentation," https://mentor.ieee.org/802.15/dcn/09/15-09-0277-07-0006-csem-fm-uwb-proposal-presentation.ppt, May 2009.

[10] J.F.M. Gerrits et al., "Principles and Limitations of Ultra-Wideband FM Communications Systems," *EURASIP J. Appl. Signal Process.*, vol. 2005 no. 3, Jan. 2005, pp. 382-396.

[11] O. Rousseaux and D. Neirynck, "Elements of an IR-UWB PHY for Body Area Networks," https://mentor.ieee.org/802.15/dcn/09/15-09-0181-03-0006-ir-uwb-phy-for-ban.pdf, Mar. 2009.

[12] K. Bynam et. al., "ETRI & Samsung PHY Proposal to 802.15.6," https://mentor.ieee.org/802.15/dcn/09/15-09-0322-01-0006-etri-samsung-phy-proposal-presentation.pdf, May 2009.

[13] J.C. Roh et al., "Texas Instruments Impulse Radio UWB Physical Layer Proposal," https://mentor.ieee.org/802.15/dcn/09/15-09-0335-00-0006-texas-instruments-impulse-radio-uwb-physical-layer-proposal.pdf, May 2009.

[14] T. Ikegami, "Meiji University UWB PHY Proposal for Body Area Network," https://mentor.ieee.org/802.15/dcn/09/15-09-0355-01-0006-meiji-university-uwb-phy-proposal-for-ban.pdf, Mar. 2009.

[15] I. Dotlić and R. Kohno, "NICT Phy Solution: Part 1: Chirp Pulse Based IR-UWB Physical Layer," https://mentor.ieee.org/802.15/dcn/09/15-09-0354-00-0006-nict-phy-solution-part-1-chirp-pulse-based-ir-uwb-physical-layer.pdf, Mar. 2009.

[16] M. Hernandez and R. Kohno, "NICT's Wideband PHY Proposal Part2: IR-UWB," https://mentor.ieee.org/802.15/dcn/09/15-09-0320-00-0006-nict-s-wideband-phy-proposal-part-2-ir-uwb.pdf, May 2009.

[17] M.Z. Win and R.A. Scholtz, "Ultra-wide Bandwidth Time-Hopping Spread-Spectrum Impulse Radio for Wireless Multiple-Access Communications," *IEEE Trans. Commun.*, vol. 48, no. 4, Apr. 2000, pp. 679-689.

[18] L. Piazzo, "Performance Analysis and Optimization for Impulse Radio and Direct-Sequence Impulse Radio in Multiuser Interference," *IEEE Trans. Commun.*, vol. 52, no. 5, May 2004,

pp. 801-810.
[19] M. Hecht and A. Guida, "Delay Modulation," *Proc. IEEE*, vol. 57, no. 1, July 1969, pp. 1314-1316.

Chengshi Zhao received the BS degree in information science and engineering from Shandong University, China, in July 2002, and the MS degree in communication and information systems from Chongqing University of Posts and Telecommunications, China, in July 2006. He is currently working toward the PhD degree with the Inha Ultra-wideband Communication Research Center (INHA UWB-ITRC), Inha University, Incheon, Korea. His research interests include cognitive radio, OFDM, MIMO, cooperative communication, and UWB techniques.

Zheng Zhou received the BS degree from Harbin Institute of Technology, Harbin, China, in 1967. He received the MS and PhD degrees from Beijing University of Posts and Telecommunications (BUPT), in 1982 and 1988, respectively. Since then, he has been with the School of Information and Communication Engineering, BUPT. From 1993 to 1995, he was a visiting research fellow with the Chinese University of Hong Kong, supported by the Hong Kong Telecom International Postdoctoral Fellowship. In 2000, he visited Japan Kyocera DDI Research Institute as an invited overseas researcher supported by The Japan Key Technology Center. He is a member of IEEE, a voting member of IEEE 802.15, and a senior member of the China Institution of Communications (CIC), the Radio Application and Management Committee of CIC, the Sensor Network Technical Committee of the China Computer Federation (CCF), and the Chinese National Technical Committee for Standardization on Radio Interference (CTCSRI/H). His research interests include short-range wireless technology, UWB wireless communications, and intelligent signal processing in telecommunications.

Kyungsup Kwak received the BS degree from Inha University, Inchon, Korea, in 1977; the MS degree from the University of Southern California in 1981; and the PhD degree from the University of California at San Diego in 1988. From 1988 to 1989, he was a member of technical staff at Hughes Network Systems, San Diego, California. From 1989 to 1990 he was with the IBM Network Analysis Center, North Carolina. Since then, he has been with the School of Information and Communication, Inha University, Korea, as a professor. He was the chairman of the School of Electrical and Computer Engineering from 1999 to 2000 and the dean of the Graduate School of Information Technology and Telecommunications from 2001 to 2002. He is now Inha Fellow Professor (IFP), and he is the current director of the Advanced IT Research Center of Inha University and the UWB Wireless Communications Research Center, Korea. Since 1994, he has served as a member of the Board of Directors, and from 2000 to 2002, he was the vice president for the Korean Institute of Communication Sciences (KICS), where he was the president in 2006. Now, he is the president of Korea Spectrum Engineering Forum, the president of Korea Institute of Intelligent Transport Systems (ITS), and the director of Korea UWB Forum. In 1993, he received the Engineering College Young Investigator Achievement Award from Inha University and a distinguished service medal from the Institute of Electronics Engineers of Korea (IEEK). In 1996 and 1999, he received Distinguished Service Medals from KICS. He received the Inha University Engineering Paper Award and the LG Paper Award in 1998 and the Motorola Paper Award in 2000. His research interests include multiple access communication systems, mobile communication systems, UWB radio systems, ad hoc networks, and sensor networks. Professor Kwak is a member of IEEE, IEICE, KICS, and KIEE.